Journal of Alloys and Compounds, 211/212 (1994) 75–79
JALCOM 077

Internal friction and substitutional–interstitial interaction in niobium-based alloys

N.P. Kushnareva and S.E. Snejko
Institute of Metal Physics, Ukrainian Academy of Sciences, Vernadsky Blvd. 36, 252142 Kiev (Ukraine)

Abstract

The logarithmic decrement δ was measured in Nb–Mo(V)–O alloys with Mo(V) content up to 50 at.% using a low frequency (f=3–7 Hz) inverse torsion pendulum in the temperature range from 20 to 700 °C. The complex δ *vs.* T curves were analysed in terms of their constituent peaks using a computer. The parameters of these peaks were used to derive information on the distribution of oxygen atoms over octahedral interstitial sites differing in the number of Mo(V) atoms contained in the surrounding nearest-neighbour lattice sites. This information was used for determining the Mo(V)–O binding energy and the structure potential barrier for oxygen atom diffusion in alloys with strong (V–O) and weak (Mo–O) interactions.

1. Introduction

The interaction between substitutional and interstitial atoms plays an essential role in the global interatomic interaction problem. Altstetter and coworkers have compared experimental results on the diffusion and thermodynamic behaviour of oxygen atoms in solid solutions of group Va metal alloys with theoretical models based on the trapping concept [1–4]. The calculated binding energies (ΔE_j) for V–O pairs are not in good quantitative agreement [1] and for Mo–O they differ qualitatively [2, 3].

The aim of this paper was to study the Mo(V)–O atom interaction in niobium alloys with up to 50 at.% Mo(V) on the basis of a Snoek peak investigation.

2. Experimental details

The alloys studied had Mo contents of 0.8, 1.5, 2.5, 3.7, 5.0, 8.0, 10, 25 and 50 at.% and V contents of 0.5, 1.0, 1.9, 7.0, 12, 20 and 50 at.%. Samples were annealed for 1 h at temperatures between 1200 and 1500 °C depending on the composition. Measurements of the logarithmic decrement δ were performed using the low frequency (3–7 Hz) torsion pendulum technique in a vacuum of 10^{-3} Pa with a temperature step of 2–3 K.

Separation of the complex curves into their constituent peaks was done using a computer programme based on the Gauss least-squares algorithm and an equation for Debye peak relaxation by inserting a set of peak j parameters (δ_{max}, T_{max} and the activation energy H). The most reliable of them were fixed, while the others were varied until the best fit with the experimental curve was achieved. The deviation of the individual peak shape from the ideal one due to broadening was taken into account using the method suggested in ref. 5.

3. Results and discussion

3.1. Nb–Mo–O system

Examples of δ–T curves and the results of their decomposition into constituent peaks for alloys with 5, 10, 25 and 50 at.% Mo are shown in Fig. 1. In unalloyed niobium T_{max} of the peak due to oxygen is 175–178 °C

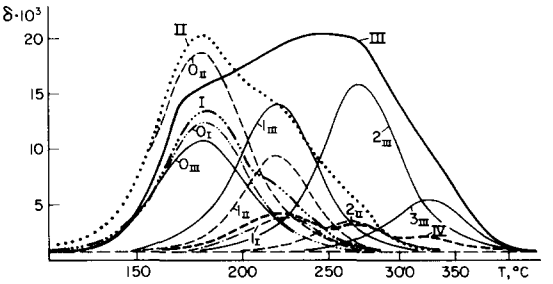

Fig. 1. δ *vs.* temperature curves for Nb alloys with 5 (I), 10 (II), 25 (III) and 50 at.% Mo (IV) (f=4 Hz) and results of their decomposition into peaks j (subscripts to peaks 0–3 indicate to which curve the peak belongs), containing 0.09 (I), 0.67 (II), 0.41 (III) and 0.04 at.% O (IV).

SSDI 0925-8388(93)00077-C

(at $f=3.5$–4.5 Hz) and $H=114$ kJ mol^{-1}. We denote this as peak 0. With an increase in Mo concentration (C_{Mo}) to 1.5–2.5 at.% the peak becomes slightly asymmetrical on the high temperature side. By analysing the shape of the curve with a computer, we identified peak 1 ($T_{max}=220$ °C) in addition to peak 0. We used a known model for the correspondence of peaks j with jumps of interstitial atoms from octahedral interstices surrounded by j substitutional atoms ($j=0$ in unalloyed niobium and 0–6 in alloys). Up to the present time such an approach has generally been accepted [6, 7], since it has firm logical grounds and leads to reasonably consistent experimental results for dilute alloys. It should be especially emphasized that different configurations of complexes with the same number j as well as diffusion paths and the existence of long-range interactions must lead to a scatter in the relaxation time τ (*i.e.* H_{maxj} values), which results in a broadening of the peaks j. These facts were confirmed by the form of the peaks due to Zr–N [6] and V–O and 2V–O complexes [7] in Nb-based alloys: these peaks did not overlap on the temperature scale and their parameters of broadening, β, were 0.4–0.8. Our results differ from the previous ones because we took into account the factors mentioned above by including the spreading of individual peaks j, $\beta=0.4$–0.8. With an increase in C_{Mo}, δ_{max1} increases as well; for the Nb–8Mo alloy peak 2 ($T_{max}=270$ °C) appears. Peaks 1, 2 and 3 ($T_{max}=320$ °C) are present for the alloy with 25 at.% Mo. For the Nb–50Mo alloy peak 0 is absent (Table 1).

The concentration of oxygen in position j (C_j) may be calculated from $C_j=K_j\delta_{maxj}$. In unalloyed Nb the coefficient K (K_0) is equal to 0.9; the values $K_{1,2,3}$ were determined as 1.0, 1.1 and 1.15 respectively. We express the quantitative data in relative units by normalizing the oxygen atom concentration in position j to that in position 0 (C_j/C_0; or C_j/C_1 for the Nb–50Mo alloy in which peak 0 is absent) (Table 2).

We have used the results of ref. 8 to evaluate the Mo–O interaction. In terms of the atomic configuration model and short-range interactions, the distribution of interstitial atoms over type j octahedral interstices, which differ in the depth of the potential energy minimum for the interstitial atoms occupying them, is defined as

TABLE 1. Parameters of peaks j in Nb–Mo–O alloys ($f=4.5$ Hz)

Parameter	$j=0$	1	2	3
T_{max} (°C)	178	220	270	324
H (kJ mol^{-1})	114	127	140	154
ΔH (kJ mol^{-1})		13	13	14

TABLE 2. Oxygen atom distribution over positions j normalized to position 0 (to position 1 for Nb–50 at.%Mo alloy) in Nb–Mo–O alloys

Composition (at.%Mo)	$j=0$	1	2	3
0	1			
1.5	1	0.01		
2.5	1	0.22		
5	1	0.26		
8	1	0.50	0.06	
10	1	0.52	0.22	
10	1	0.53	0.17	
25	1	1.54	1.78	0.55
50		1.00	0.58	0.35

TABLE 3. Experimental energies of Mo–O interaction in Nb–Mo–O alloys

Composition (at.%Mo)	C_1/C_0	ν_1/ν_0	ΔE_1 (kJ mol^{-1})
2.5	0.22	0.15	−1.49
5	0.26	0.32	0.73
8	0.50	0.53	0
10	0.52	0.67	0.98
25	1.54	2.14	1.37
	C_2/C_0	ν_2/ν_0	ΔE_2 (kJ mol^{-1})
10	0.16	0.19	0.59
10	0.22	0.19	−0.69
25	1.78	1.69	−0.24
	C_3/C_0	ν_3/ν_0	ΔE_3 (kJ mol^{-1})
25	0.55	0.75	1.59

$$C_j=\frac{h_j\exp(-E_j/kT)}{\sum_{n=1}^{m}h_n\exp(-E_n/kT)} \quad (1)$$

where E_j and E_n are the atom potential energies in the jth and nth positions respectively and h_j and h_n are the relative concentrations of interstices of types j and n respectively. Taking eqn. (1) into account, we obtain

$$\frac{C_j}{C_0}=\frac{h_j}{h_0}\exp\left(-\frac{\Delta E_j}{kT}\right) \quad (2)$$

where $\Delta E_j=E_j-E_0$ is the binding energy for Mo–O complexes in Nb.

In refs. 8 and 9 h_j was found to be

$$h_j=\frac{\nu_j}{\nu}=\frac{6!}{j!(6-j)!}C_A^j(1-C_A)^{6-j} \quad (3)$$

where ν is the total number of octahedral interstices, ν_j is the number of type j interstices and C_A is the concentration of substitutional solute, C_{Mo} in our case.

Table 3 lists the values of ΔE_1 estimated according to eqn. (2), based on the data C_1/C_0 (see Table 2). Values of ΔE_1 and ΔE_3 are positive as a rule, which

indicates a weak repulsion between Mo–O and 3Mo–O atoms in Nb. The Mo–O–Mo configuration is more stable: in accordance with the experimental spread, the average value of ΔE_2 is close to zero.

Hence Mo atoms are antitraps for oxygen atoms, while at the same time the latter have a higher diffusion activation energy when they are located near Mo atoms.

3.2. Nb–V–O system

Only peak 1 ($T_{max}=280$ °C, $f=4$ Hz) is revealed in the δ *vs.* T curve for the Nb–0.5at.%V alloy with C_O below 0.5 at.%, in agreement with the results of refs. 6, 7, and 10. When C_O becomes higher than C_V, peak 0 appears, confirming the results of ref. 7. For the Nb–1.9V alloy, in addition to peak 1, peak 2 ($T_{max}=415$–420 °C) is seen (Fig. 2, curves I–III) and for samples with $C_O>0.08$ at.% peak 3 appears ($T_{max}=365$–370 °C).

In annealed samples of the Nb–7V alloy the oxygen relaxation is practically absent, while after oxidation four peaks are seen in curve IV (Fig. 2), *i.e.* peaks 1, 2, 3 and 4 (at 320–325 °C). It can be seen that peak 1 is the largest for the alloy with 1.9 at.% V, while for the alloy with 7 at.% V peak 2 is the largest. Four peaks (1, 2, 3 and 4) are present in the curves for 12, 20 and 50 at.% V. The relationship between their δ_{max} values depends on C_V but not on C_O. The oxygen atom distribution over the position j tends to the statistical one with an increase in C_V of the alloy. Examples of curves for the Nb–50V alloy with two values of C_O are shown in Fig. 3.

The results presented above do not agree with the results of ref. 7, where one broad peak was found for the Nb–10V alloy with T_{max} somewhat higher than T_{max2}. This peak was assumed to be caused by the reorientation of oxygen atoms associated with two or more V atoms. We believe and have experimental evidence that the authors were dealing in that case mainly with nitrogen relaxation. The parameters (T_{max} and H_{max}) of peaks

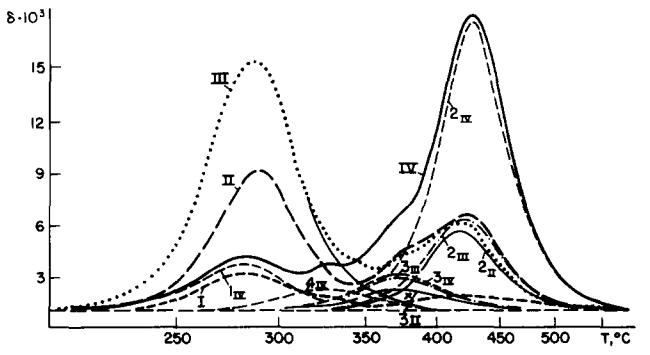

Fig. 2. Temperature dependence of δ and results of δ curve decomposition into peaks j for Nb alloys with 1.9 (I–III) and 7 at.% V (IV). Oxygen concentrations C_O (at.%): I, 0.05; II, 0.24; III, 0.30; IV, 0.50.

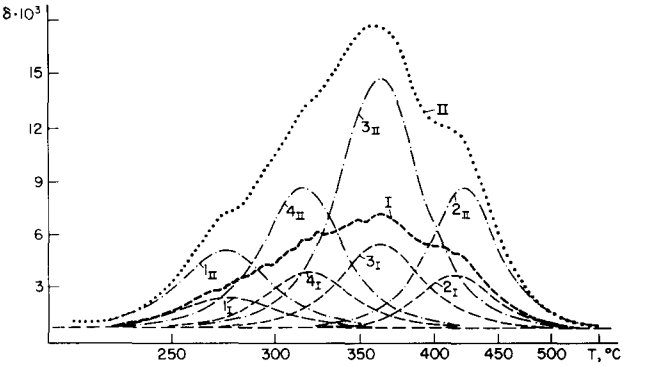

Fig. 3. δ *vs.* temperature curves and their decomposition into peaks j for Nb–50at.%V alloy with 0.25 (I) and 0.60 at.% O (II).

TABLE 4. Parameters of peaks j in Nb–V–O alloys ($f=4$ Hz)

Parameter	$j=0$	1	2	3	4
T_{max} (°C)	178	285	420	370	325
H (kJ mol^{-1})	114	142	179	164	153
ΔH (kJ mol^{-1})		28	37	−15	−9

TABLE 5. Experimental energies of V–O interaction in Nb–V–O alloys

Composition (at.% V)	C_1/C_0	ν_1/ν_0	ΔE_1 (kJ mol^{-1})
0.5	3×10^2	0.03	−42.2
0.5	3×10^3	0.03	−52.8
1.0	5.4×10^2	0.06	−41.7
1.0	5.4×10^3	0.06	−52.3
	C_2/C_1	ν_2/ν_1	$\Delta E_{(2-1)}$ (kJ mol^{-1})
1.9	0.573	4.82×10^{-2}	−14.0
1.9	0.758	4.82×10^{-2}	−15.5
5.0	2.167	0.1315	−15.8

j for Nb–V–O alloys are given in Table 4. Table 5 lists the estimated binding energies of V–O atoms in Nb–V–O alloys. Because peak 0 is absent for the Nb–0.5V alloy, we assumed that δ_{max0} is equal to the background damping at the corresponding peak temperature. In this case ΔE_1 is −42.2 kJ mol^{-1}. If δ_{max0} is taken to be one order of magnitude lower, then ΔE_1 is −52.8 kJ mol^{-1}. The same ΔE_1 values were obtained for the Nb–1at.%V alloy. Comparison of these results with the binding energies for the Nb–V–O system obtained from equilibrium and diffusion experiments and summarized in ref. 1 shows the best agreement to be with the value of −46.7 kJ mol^{-1} for the Nb–2.7V alloy obtained from equilibrium experiments (thermodynamic activity measurements). The values of $\Delta E_{(2-1)}=E_2-E_1$ calculated on the basis of the present results for the

Nb–1.9at.%V alloy and using the results for Nb–5V (see Table 5, last row) from ref. 7 (Fig. 3, curve 4 of Ref. 7) coincide well and are equal to -15.5 kJ mol^{-1}. Thus, if we set ΔE_1 equal to -46 kJ mol^{-1}, then ΔE_2 is -61 kJ mol^{-1}. The $\Delta E_{(j-1)}$ values calculated for the Nb–50V alloy based on the results of Fig. 3 are 0 ± 1.5 kJ mol^{-1}. This means that the oxygen atom distribution over positions j in the Nb–50V alloy is close to the fractions of these type j interstices, *i.e.* close to the statistical distribution.

The data presented above allow us to propose the scheme of interstitial atom energy variations in systems with traps (Nb–V–O) and antitraps (Nb–Mo–O) shown in Fig. 4. In this case the energy H required for an atom i to jump from a trap (antitrap) to a normal site is

$$H = H_{\text{norm}} - \Delta E_j - \Delta E' \quad (4)$$

where H_{norm} ($H_{\max}$ in Nb–O alloy) is 114 kJ mol^{-1}. In the Nb–V–O system ΔE_1 is -46 kJ mol^{-1} and $H_{\max 1} = 142$ kJ mol^{-1}; thus $\Delta E'$ is calculated as 18 kJ mol^{-1}. That is, the reorientation of oxygen atoms from one trap to a neighbouring one around V atoms in internal friction experiments takes place via the overcoming of the potential barrier lowered by $\Delta E'_t$ (18 kJ mol^{-1}). The activation energy for oxygen atom diffusion in the Nb–0.5V alloy has been determined as 176 ± 9 kJ mol^{-1} [11], which exceeds $H_{\text{norm}} - \Delta E_j$ by 16 kJ mol^{-1}. Therefore, to escape from traps (the condition necessary for macrodiffusion to take place), the barrier is higher by $\Delta E'_{\text{esc}}$; in the present case $\Delta E'_{\text{esc}} = -16$ kJ mol^{-1}. For type 2 traps (2V–O) with $\Delta E_2 = -61$ kJ mol^{-1} and $H_{\max 2} = 179$ kJ mol^{-1}, $\Delta E'_t = -4$ kJ mol^{-1} (*i.e.* the barrier has increased). As can be seen from Fig. 4, the difference between H_{dif} and $H_{\max}$ is $E'_t - \Delta E'_{\text{esc}}$. In the Nb–Mo–O system, where $\Delta E_j > 0$, the increase in jump activation energy can only be due to the growth of $\Delta E'$ (Fig. 4(b)). It follows from Table 1 that $H_{\max}$ of each successive peak up to peak 3 increases by $\Delta H = 13$–14 kJ mol^{-1}, so we can write $H_{\max j} = H_{\text{norm}} + j\Delta H$, ignoring ΔE_j values that have low moduli. In this case $\Delta E'$ coincides with $\Delta E'_{\text{esc}}$, which is why the activation energies from internal friction and macrodiffusion measurements correlate. Thus the distribution of atoms i over positions j ($\delta_{\max j}$) in internal friction experiments gives the possibility of evaluating the binding energies ΔE_j (appropriate for equilibrium measurements), whereas $H_{\max j}$ ($T_{\max j}$) contains information about the energy barrier for jumps and includes the saddle point energy change $\Delta E'$ (appropriate for dynamic diffusion experiments). Therefore correlation between H_{dif} and $H_{\max}$ takes place only in alloys with weak interactions, otherwise H_{dif} exceeds $H_{\max}$.

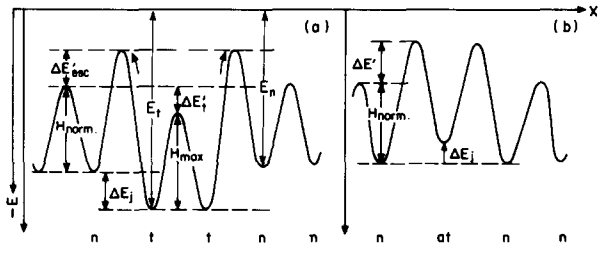

Fig. 4. Representation of the free activation energies for jumps of atoms i in systems with (a) traps ($\Delta E_j < 0$) and (b) antitraps ($\Delta E_j > 0$). $\Delta E_j = E'_t - E_n$; H_{norm} is the potential barrier between normal interstices; $\Delta E'$ is the change in saddle point energy.

4. Conclusions

(1) The distribution of oxygen atoms over octahedral interstices differing in the number j of nearest-neighbour Mo(V) atoms was obtained by a Snoek relaxation investigation of niobium-based alloys. Comparing the obtained distribution with the fractions of positions j leads to the calculation of the Mo(V)–O binding energies ΔE_j.

(2) A small absolute value of $\Delta E_{\text{Mo–O}}$ (0–1.4 kJ mol^{-1}) and a positive sign correspond to weak repulsion between Mo–O atoms at 150–400 °C, which changes slightly for complexes with $j = 1, 2, 3$.

(3) The increase in $H_{\max}$ of peaks j in alloys with weak interaction is determined by the change in the saddle point energy for oxygen atom jumps and $H_{\max}$ coincides with H_{dif}.

(4) There is a strong interaction of a chemical nature between V–O atoms in Nb–V–O alloys with up to 5 at.% V which is determined by the binding energy ($\Delta E_{\text{V–O}} = -46$ kJ mol^{-1}, $\Delta E_{\text{2V–O}} = -61$ kJ mol^{-1}). The potential barrier for oxygen atom reorientation around V traps ($H_{\max}$) is lowered while that for escaping from traps (H_{dif}) is raised by a decrease and an increase in the saddle point energy respectively, so that $H_{\max}$ does not coincide with H_{dif}.

(5) The attraction inside jV–O complexes for $j \geqslant 3$ is markedly weakened, local action is lost and the oxygen atom distribution with an increase in the vanadium concentration approaches the statistical one.

(6) The reasons for the inadequacy of most models are ignoring the change in the saddle point energy for dynamic diffusion processes, taking into account traps of only one type and assuming the equivalence of H_{dif} and $H_{\max}$ for all systems.

References

1 J. Park and C.J. Altstetter, *Acta Metall.*, *34*(1) (1986) 2217–2224.
2 J.S. Lee and C.J. Altstetter, *Acta Metall.*, *34*(1) (1986) 131–138.
3 J.S. Lee and C.J. Altstetter, *Acta Metall.*, *34*(1) (1986) 139–145.
4 R.J. Lauf and C.J. Altstetter, *Acta Metall.*, *27* (1979) 1157–1163.

5 N.P. Kushnareva and V.M. Pechersky, *Zavodsk. Lab.*, (4) (1989) 47–48.
6 Z.C. Szkopiak and J.T. Smith, *J. Phys. D: Appl. Phys., 8* (1975) 1273–1284.
7 H. Indrawirawan, O. Buck and O.N. Carlson, *Phys. Status Solidi A, 104* (1987) 443–451.
8 A.A. Smirnov, *Theory of Interstitial Alloys,* Nauka, Moscow, 1979.
9 M. Barabash, Study of phase equilibria, structure and strength properties of the vanadium, niobium and molybdenum alloys with refractory nitrides, *Abstract of Dissertation,* Kiev, 1975.
10 O.N. Carlson, H. Indrawirawan, C.V. Owen and O. Buck, *Metall. Trans. A, 18* (1987) 1415–1420.
11 M.D. Treng, H. Indrawirawan and O.N. Carlson, *J. Less-Common Met., 136* (1987) 31–39.